Strojniški vestnik - Journal of Mechanical Engineering 62(2016)9, 521-533

DOI:10.5545/sv-jme.2016.3482 Original Scientific Paper
Received for review: 2016-02-03
Received revised form: 2016-05-06
Accepted for publication: 2016-05-09

Numerical Investigation of the Nanoparticle Volume Fraction Effect on the Flow, Heat Transfer, and Entropy Generation of the Fe_3O_4 Ferrofluid under a Non-uniform Magnetic Field

Fazel Hosseinzadeh[1] – Faramarz Sarhaddi [1,*] – Davod Mohebbi-Kalhori[2]
[1] University of Sistan and Baluchestan, Department of Mechanical Engineering, Iran
[2] University of Sistan and Baluchestan, Department of Chemical Engineering, Iran

This paper presents research on the forced flow convective heat transfer of a ferrofluid (water and Fe_3O_4) in a horizontal two-dimensional channel under the influence of a 2D non-uniform magnetic field, which is applied through a line dipole. The governing equations of this research include continuity, momentum, energy and entropy generation, which are solved with a finite volume technique. Moreover, a grid-independent test and the validation of numerical results are carried out. The effect of the Fe_3O_4 volume fraction (1 vol % to 6 vol %) on the hydro-thermal characteristics of the ferrofluid flow and entropy generation is studied. Numerical results show that the flow pattern is highly changed, because the kelvin body force overcomes the viscous force by increasing the volume fraction under applied magnetic field. Furthermore, the average wall friction factor increases linearly. The average Nusselt number ($\overline{Nu}$) increases with the increase of the Fe_3O_4 volume fraction, so that $\overline{Nu}$ increases by 51.1 % in comparison to the base fluid at 6 vol %. It is observed that the Nusselt number ratio (NUR) at 6 vol % is enhanced by 10.4 % whereas the entropy generation ratio (NSR) is increased by only 6.2 % compared to 4 vol %. According to the results of the study, it is concluded that using volume fractions between 4 vol % to 6% would result in an observable improvement in convective heat transfer while enhanced entropy generation is relatively small, so it is thermodynamically affordable.

Keywords: ferrofluid, nanoparticle volume fraction, magnetic field, entropy generation, finite volume

Highlights

- *This paper represents a numerical investigation of laminar forced ferrofluid flow.*
- *A line diploe was used to generate the non-uniform external magnetic field.*
- *The effect of the Fe_3O_4 volume fraction on the hydro-thermal parameters has been investigated.*
- *As the external magnetic field is applied, the kelvin body force overcomes the viscous force.*

0 INTRODUCTION

Ferrofluids are colloidal suspensions comprised of a non-magnetic carrier liquid such as water, hydrocarbon oils or kerosene, and the single-domain ferromagnetic nanoparticles. They appear useful in heat transfer applications and other fields of practice. The magnetic behaviour of the ferrofluid is due to the magnetic nature of the solid phase spread into the liquid. The particles are usually 10 nm large, and they have bipolar magnets; an applied magnetic field causes them to take the same direction as the magnetic field lines and form a unique magnetic domain. To prevent the mixture from the aggregation that is caused by the existing magnetic forces between the particles while producing ferrofluid, they are coated with a 2 nm layer of liquid surfactant **[1]**. Ferrofluids have significant potential to alter the flow field through changing the magnetic field due to the bilateral effects of the fluid's nature and the magnetic properties of particles. Moreover, for every case-specific application, it is possible to regulate the magnetic force applied to the ferrofluid via an appropriate design of the external magnetic field. Ferro-hydrodynamic characteristic lengths differing from micro- to nano-scales bring a wide range of novel applications in the various fields of study **[2]**, including thermal engineering **[3]** and bio-engineering **[4]**. The transport of water in nanoconfined geometries is different than in the bulk phase and has tremendous implications in nanotechnology and biotechnology **[5]**. Using electromagnetic fields for micro-fluid applications presents a new method for controlling the ferrofluid **[6]**. Some applications such as pumping and mixing of the fluid in the micro-dimension apparatuses are possible through the electromagnetic body force (Lorentz force). The Lorentz force is created by an interaction between a magnetic field and an electric current, which is usually provided externally **[7]**. As the heat and momentum transfer are limited to small apparatuses, using an external magnetic field can improve the convective heat transfer characteristics inside them. This issue becomes significant in devices working based on free convection heat transfer for which the dimensions of the geometry are tiny, or the effect of gravity is negligible. Furthermore, with increasing interest in micro-scale heat exchangers used in microelectromechanical systems (MEMS)

*Corr. Author's Address: Department of Mechanical Engineering, University of Sistan and Baluchestan, Zahedan, Iran, fsarhaddi@eng.usb.ac.ir

systems, the application range of ferrofluids has risen considerably. To have an optimal design and a handy control over thermomagnetic heat transfer applications, it is essential to determine the relationship between the applied magnetic field, the ferrofluid flow, and temperature distribution.

Finlayson [8] investigated thermomagnetic convection heat transfer and analytically computed a parameter for the critical stability of this type of convection. Tangthieng et al. [9] numerically investigated the heat transfer of ferrofluid flow between two flat plates and within a square enclosure subjected to a steady magnetic field. Their results indicated that heat transfer caused by the magnetic field gradient is increased significantly. Tzirtzilakis et al. [10] worked on the flow of a biological magnetic fluid in a 3D rectangular duct. Assuming a viscous, laminar, incompressible and developed flow, they simulated a nonconductor biomagnetic fluid under the influence of an external magnetic field. Their research showed that the flow is considerably affected by the magnetic field. Ganguly et al. [2] conducted research on the heat and mass transfer in ferrofluids with application in the MEMS and biomedicine. Their final results suggested that the effect of the external field is nude unless kelvin force overcomes viscous force and heat transfer increases with the strengthening of the magnetic field. Jafari et al. [11] simulated heat transfer of the kerosene-based ferrofluid using a CFD method inside a cylindrical geometry with a two-phase mixture model. They used a range of temperature gradients and magnetic fields. They showed that transfer phenomena increase in the presence of magnetic field. They also demonstrated that, when magnetic particles are aggregated, heat transfer decreases. They concluded that magnetic fields perpendicular to the temperature gradient cause a greater deal of heat transfer in comparison to that of a parallel situation. Lajvardi et al. [12] carried out an experimental investigation on the convective heat transfer of a ferrofluid flowing through a heated copper tube under an applied magnetic field. A significant increase in the amount of heat transfer by applying magnetic field was observed in their experiments. In addition, they examined the effect of magnetic nanoparticle concentration and the magnet position. Their examinations suggested that the main reason behind the increase of heat transfer coefficient is owing to the considerable enhancement in thermo-physical properties of the ferrofluid, which happens because of applying the magnetic field. Aminfar et al. [13] numerically investigated the hydrothermal behaviour of a ferrofluid (water and 4 vol % magnetite) in a rectangular vertical duct using two-phase mixture model and control volume technique under the influence of a transverse magnetic field. Their results showed that applying magnetic fields increases the Nusselt number and friction factor and also creates a pair of vortices, which prevents nanoparticles from aggregating and enhances heat transfer. Afrand et al. [14] investigated the effect of the magnetic field intensity, the Hartmann number, the Rayleigh number, the angle of magnetic field application, the ratio of the inner to outer radii of the annulus on the flow, and the temperature field of molten gallium in a long annulus between two horizontal cylinders. They found that with an increase in the Rayleigh number, the change in Nu with the magnetic field intensity does not occur. Natural convection of an electrically conducting fluid in a tilted cylindrical annulus under the influence of a magnetic field was carried out numerically by the same team of researchers [15]. They showed that the effect of the transverse magnetic field is more significant than that of the axial magnetic field on the average Nusselt number. In another work, Afrand et al. [16] performed 3D numerical simulation and multi-objective optimization of natural convection in a cylindrical annulus mould filled with molten potassium under a magnetic field. Mahmoodi et al. [17] studied magneto-hydrodynamic (MHD) natural convection fluid flow and heat transfer in a square enclosure filled with liquid gallium with a pair of source and sink on its walls. They investigated the effects of the Rayleigh number, the Hartman number, and the locations of the source and sink on the fluid flow and heat transfer inside the enclosure. Their results showed that the flow and temperature distributions inside the enclosure are affected by the strength of the magnetic field, the Rayleigh number, and the relative location of the heat source and sink. Malvandi et al. [18] investigated MHD mixed convection of alumina/water nanofluid inside a vertical annular pipe. They used a model for the nanofluid mixture involving Brownian motion and thermophoresis diffusivities in order to take into account the effects of nanoparticle migration. They showed that the advantage of nanofluids in heat transfer enhancement was reduced in the presence of a magnetic field. Recently Goshayeshi et al. [19] through an experimental work studied the effect of Fe_2O_3/Kerosene nanofluid to the copper closed-loop oscillating heat pipe under the magnetic field for inclination angles ranging from 0° to 90°, under different heat inputs (10 W to 90 W). They showed that Fe_2O_3 nanoparticles could improve the thermal resistance and subsequently thermal performance as

well as the pipe's heat transfer coefficient, especially under the magnetic field.

The problem of entropy generation has attracted a great deal of attention in various engineering applications including heat exchangers, turbo machinery, electronic cooling systems, combustion engines, etc.

Thermodynamic irreversibility is related to entropy generation as a phenomenon appearing in every heat transfer Process. Various factors such as heat transfer and viscous losses affect the entropy generation. Bejan **[20]** studied entropy generation due to the heat transfer and fluid viscosity as an objective function for geometry optimization of pipes in a heat exchanger. He showed that entropy generation in forced flow convective heat transfer is due to temperature gradient and viscous effects of the fluid. Ibanez et al. **[7]** optimized an MHD fluid flowing through two infinite parallel plates of limited conductivity by means of the entropy minimization method. They aimed to minimize the total energy loss caused by irreversibilities, which are due to several factors including thermal conductivity, viscous losses, and the Joule dissipations. Thus, they analytically solved velocity, temperature and electric current density fields for computing total entropy generation in terms of the dimensionless parameters of the problem. They demonstrated that with decreasing wall temperatures, entropy generation reaches a minimum value. Mahian et al. **[21]** analytically studied the first and the second laws of thermodynamics for MHD flow between two rotating cylinders and investigated the effect of MHD flow on the velocity, temperature and entropy generation distribution between them. They investigated the effect of the Hartman number, Brinkman number and radius ratio on the entropy generation. Their investigation suggested that increasing the Hartman number, results in increasing average entropy generation. Rashidi et al. **[22]** studied effects of magnetic interaction number, slip factor and relative temperature difference on velocity and temperature profiles as well as entropy generation in MHD flow of a fluid with variable properties over a rotating disk using numerical methods. Recently Mojumder et al. **[23]** numerically analysed magneto-hydrodynamic convection in a half-moon shaped cavity filled with ferrofluid. They used cobalt-kerosene and Fe_3O_4-water ferrofluids for their investigation. They concluded that the entropy generation is increased with the increment of *Ra*, the decrement of *Ha* and a moderate inclination angle (γ = 45°). They found that ferrofluid always causes higher entropy generation and at the same time higher heat transfer rate. Finally, they suggested that the optimum value of solid volume fraction of ferrofluid should be used to optimize the entropy and to enhance the heat transfer simultaneously. However, there is no significant research into entropy generation caused by temperature difference, friction factor and energy losses in ferrofluids. Although, owing to the wide range of ferrofluid applications in industry, the entropy generation investigation can be beneficial and may provide basic knowledge for selecting design parameters in systems of such type. Furthermore, studying thermal and hydrodynamic parameters and entropy generation in ferrofluids seems to be essential for recognizing and eliminating or optimizing the leading causes of energy losses in the system. This research studies the effect of Fe_3O_4 volume fraction on the flow, heat transfer and entropy generation of the water-Fe_3O_4 ferrofluid through numerical investigation.

The problem chosen in this study is supposed to have a small geometry (millimetre order) with low Reynolds numbers. The domain of applications related to this problem is comprehensive, for example in small devices like MEMS, heat exchangers and cooling systems for electronic devices as a possible alternative for natural convection.

1 PROBLEM DESCRIPTION AND GOVERNING EQUATIONS

The main target in the present work is to investigate the effect of Fe_3O_4 volume fraction as the magnetic nanoparticle with a diameter of 10 nm on the hydro-thermal parameters and entropy generation of the ferrofluid. The geometry in which the ferrofluid flows is a two-dimensional rectangular channel (20 mm × 2 mm) in the axial and transverse directions, respectively). The effect of gravitation is neglected due to the small geometry. A line dipole with a dipole strength of 0.1 Am is placed 1 mm below the lower channel wall halfway along the channel length, acting as the external 2D magnetic field. Heated ferrofluid at characteristic Reynolds number Re=20, enters the channel with the temperature of 344 K. The lower wall is considered to be an isothermal heat sink at 300 K, while the upper wall is adiabatic (Fig. 1). The laminar ferrofluid flow is assumed to be steady state, incompressible, and viscous. The effect of the magnetic field on the viscosity and thermal conductivity of the ferrofluid is not considered, and the Lorentz force caused by electric conductivity has been neglected in comparison to the magnetization.

The Knudsen number is given by $Kn=\lambda/L_s$ where λ is the mean free path in a gas and L_s is the

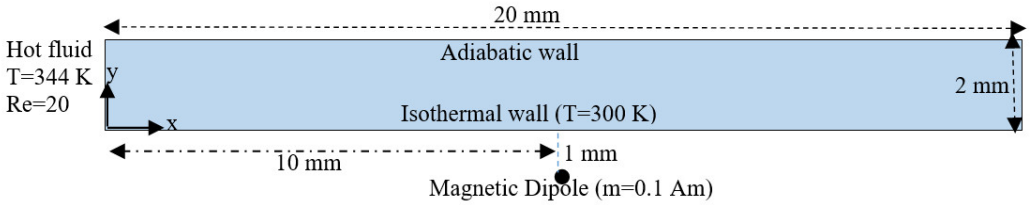

Fig. 1. *Schematic diagram of the physical model*

characteristic channel length. For liquids, the lattice spacing δ can be used as an alternative to mean free path. For water, this spacing is 0.3 nm [24]. In this work L_s is the channel height; therefore, the Knudsen number is approximately about 1.5×10^{-7}, and the continuum flow assumption is satisfied.

Considering all the aforementioned assumptions, the governing equations of the problem are as follows:

- continuity equation:

$$\nabla\cdot\boldsymbol{V}=0, \tag{1}$$

- momentum equation:

$$\rho_{eff}\nabla\cdot(\boldsymbol{VV})=-\nabla p+\nabla\cdot\left(\mu_{eff}\nabla\boldsymbol{V}\right)+(\boldsymbol{M}\cdot\nabla)\boldsymbol{B}, \tag{2}$$

where **V** is the velocity vector, ρ_{eff} is ferrofluid's density and μ_{eff} is effective viscosity. The last term in Eq. (2) $(\boldsymbol{M}\cdot\nabla)\boldsymbol{B}$ is called Kelvin body force. This force is owing to the existence of the magnetic gradient. As it is assumed that the ferrofluid does not conduct electric current, Maxwell's equations are obtained as:

$$\nabla\cdot\boldsymbol{B}=0, \tag{3}$$

and

$$\nabla\times\boldsymbol{H}=0. \tag{4}$$

In Eqs. (3) and (4), $\boldsymbol{B}$ and $\boldsymbol{H}$ are magnetic induction and magnetic field intensity, respectively. If we define $\boldsymbol{M}$ as the magnetization created inside the ferrofluid, $\boldsymbol{B}$, $\boldsymbol{M}$, and $\boldsymbol{H}$ are related to each other through $\boldsymbol{B}=\mu_0(\boldsymbol{M}+\boldsymbol{H})$. When a ferrofluid is exposed to an external magnetic field, magnetic dipoles of nanoparticles become aligned with the direction of the external field vectors. The magnitude of magnetization is a function of the external magnetic field and temperature [8] and [25]:

$$\boldsymbol{M}=M(H,T)\frac{\boldsymbol{H}}{H}, \tag{5}$$

where T is the temperature, $H=|\boldsymbol{H}|$ is the magnitude of the applied magnetic field, and $M=|\boldsymbol{M}|$ is the value of magnetization created inside the ferrofluid [25]. According to Aminfar et al. [13], magnetization is defined as follows:

$$M=M_sL(\xi)=\frac{6m_p\varphi}{\pi d_p^3}\left(\coth(\xi)-\frac{1}{\xi}\right). \tag{6}$$

In Eq. (6), M_s is the saturated magnetization of the particles, φ is the volume fraction of magnetic particles, m_p is the particle magnetic moment, d_p is diameter, and ξ is the Langevin parameter. A unit cell of the crystal structure of magnetite (Fe_3O_4) has a volume of 730 Å^3 and includes 8 molecules of Fe_3O_4, each of which has a magnetic moment of $4\mu_B$. The magnetic moment of magnetite particles is then obtained from Eq. (7):

$$m_p=\frac{4\mu_B\pi d_p^3}{6\times91.25\times10^{-30}}. \tag{7}$$

Langevin parameter is the ratio of magnetic energy to thermal energy which is given by:

$$\xi=\frac{\mu_0m_pH}{k_BT}, \tag{8}$$

where μ_B is the Bohr magneton which equals 9.27×10^{-24} (Am^2) in SI system. The other parameter k_B, is the Boltzmann's constant, which relates the energy level of particle and its temperature. This value is the relative magnitude of the universal gas constant and Avogadro number which equals 1.3806503×10^{-23} J/K. Langevin's function is used to describe the competent behaviour between disordering (random thermal), and ordering (magnetic torque) mechanisms [1] and is defined by Eq. (9):

$$L(\xi)=\coth(\xi)-\frac{1}{\xi}. \tag{9}$$

External magnetic field components made by line dipole in x and y directions are H_x and H_y which are defined through Eqs. (10) and (11), respectively.

$$H_x(x,y)=\frac{2m(x-a)(y-d)}{(x-a)^2+(y-d)^2}, \tag{10}$$

and

$$H_y(x,y)=\frac{m\left[(y-d)^2-(x-a)^2\right]}{(x-a)^2+(y-d)^2}. \tag{11}$$

In Eqs. (10) and (11), m is the magnetic dipole strength per unit length of the electromagnetic coil, which is defined as $m=Ib/2\pi$, I is electric current inside the coil, b is the distance between the conductors, and (a,d) represents the coordinates of the dipole. The magnitude of the magnetic field is computed in Eq. (12):

$$H(x,y)=\frac{m}{(x-a)^2+(y-d)^2}. \quad (12)$$

Through defining magnetic susceptibility as $\chi_m=\boldsymbol{M}/\boldsymbol{H}$, the relationship between magnetization and the external magnetic field becomes:

$$\boldsymbol{M}=\frac{M_s L(\xi)}{H}\boldsymbol{H}=\chi_m \boldsymbol{H}. \quad (13)$$

Magnetic susceptibility of ferrofluid is a dimensionless number that depends on the temperature and the applied magnetic field. Substituting Eq. (13) into Eq. (5), we obtain:

$$\boldsymbol{B}=\mu_0(1+\chi_m)\boldsymbol{H}. \quad (14)$$

Eq. (14) correlates magnetic induction into ferrofluid with the applied magnetic field. The energy equation for incompressible and steady state ferrofluid flow assuming single phase model is as follows [8]:

$$\left[(\rho C_p)_{nf}-\mu_0 \boldsymbol{H}\cdot\left(\frac{\partial M}{\partial \mathrm{T}}\right)_H\right]\boldsymbol{V}.\nabla T+$$
$$+\mu_0 T\left(\frac{\partial \boldsymbol{M}}{\partial T}\right)_H\cdot(\boldsymbol{V}\cdot\nabla\boldsymbol{H})=\nabla\cdot(k_{nf}\nabla T)+\mu_{nf}\Phi, \quad (15)$$

where Φ is the loss function that expressed as below:

$$\Phi=2\left[\left(\frac{\partial u}{\partial x}\right)^2+\left(\frac{\partial v}{\partial y}\right)^2\right]+\left[\left(\frac{\partial u}{\partial y}+\frac{\partial v}{\partial x}\right)^2\right]. \quad (16)$$

The entropy generation equation in the absence of electrical effects is as follows [26]:

$$S_G=\frac{k_{eff}}{T_0}(\nabla T)^2+\frac{\mu_{eff}}{T_0}\Phi. \quad (17)$$

The ferrofluid's physical properties in the aforementioned equations are as below:

- ferrofluid's density:

$$\rho_{eff}=\varphi\rho_p+(1-\varphi)\rho_f, \quad (18)$$

- dynamic viscosity [27]:

$$\mu_{eff}=\mu_f(1+2.5\varphi+6.5\varphi^2), \quad (19)$$

- effective thermal conductivity for spherical nanoparticles [28]:

$$k_{eff}=\frac{k_p+2k_f-2\varphi(k_f-k_p)}{k_p+2k_f+\varphi(k_f-k_p)}k_f, \quad (20)$$

- effective specific heat:

$$(\rho C_p)_{eff}=(1-\varphi)(\rho C_p)_f+\varphi(\rho C_p)_p. \quad (21)$$

1.1 Boundary Conditions

The governing equations have been subjected to the following boundary conditions:

- At the inlet (i.e. $x/h=0$), hot ferrofluid enters with a temperature of T_h at characteristic Reynolds $\mathrm{Re}=20$:

$$\frac{x}{h}=0,\quad u=u_\infty,\quad v=0,\quad T=T_h. \quad (22)$$

- At the lower wall, the non-slip condition is established and imposed at constant cold temperature of T_c:

$$\frac{y}{h}=0,\quad u=v=0,\quad T=T_c. \quad (23)$$

- There is a non-slip condition on the upper wall, which is considered to be adiabatic:

$$\frac{y}{h}=1,\quad u=v=0,\quad \frac{\partial T}{\partial y}=0. \quad (24)$$

- At the outlet (i.e. $x/h=10$), the atmospheric pressure is assumed.

2.3 Dimensionless Parameters

In order to investigate hydrodynamic and thermal behaviour, as well as entropy generation in the ferrofluid in the present work, the dimensionless numbers of friction factor on the lower wall, Nusselt number, dimensionless temperature, and entropy generation is defined as follows:

The Reynolds number is the ratio of inertial forces to viscous forces and defined as below:

$$\mathrm{Re}=\frac{\rho_{eff}u_\infty h}{\mu_{eff}}. \quad (25)$$

The Nusselt number is defined as the ratio of convective heat transfer into heat transferred by conduction in system boundaries. The local Nusselt number on isothermal wall is given by:

$$Nu = \frac{q_w^{"} h}{k_{eff}\left(T_b - T_c\right)}, \tag{26}$$

where T_b in is the bulk temperature of ferrofluid flow which is obtained as:

$$T_b = \frac{\int_0^h uTdy}{\int_0^h udy}. \tag{27}$$

The average Nusselt number is obtained by the integration of Eq. (28) in the longitudinal direction.

$$\overline{Nu} = \frac{1}{L}\int_0^L Nu\, dx. \tag{28}$$

The friction factor on the bottom wall can be achieved from Eq. (30).

$$C_f = \frac{\tau_w}{\frac{1}{2}\rho_{eff} u_\infty^2}, \tag{29}$$

where:

$$\tau_w = \mu_{eff} \left.\frac{\partial u}{\partial y}\right|_{wall}. \tag{30}$$

Dimensionless entropy generation number:

$$Ns = \frac{S_g}{S_{g0}}, \tag{31}$$

where, S_{g0} is the characteristic entropy generation rate [29]:

$$S_{g0} = k_{eff}\left(\frac{\Delta T}{hT_0}\right)^2. \tag{32}$$

In Eq. (32), $\Delta T = T_h - T_c$ and T_0 is the reference temperature which is 300 K. the average entropy generation rate is obtained by integrating Eq. (31) over the whole volume from the Eq. (33) given below:

$$\overline{Ns} = \frac{1}{\forall}\int_{\forall} Nsd\forall, \tag{33}$$

where $\forall$ presents the volume of the whole channel.

Dimensionless temperature:

$$\theta_b = \frac{T_b - T_c}{T_h - T_c}. \tag{34}$$

2 NUMERICAL METHOD

Because of the non-linearity of coupled governing differential equations, the numerical method was chosen to solve them. The control volume technique was applied to discretize continuity, momentum and energy equations. For convective and diffusive terms, a second order upwind method was applied while a simple algorithm was developed for pressure-velocity coupling. A structured grid has been used to discretize the computational domain (Fig. 2). As can be seen, the grid is finer near the dipole, because of higher gradient amounts in this area.

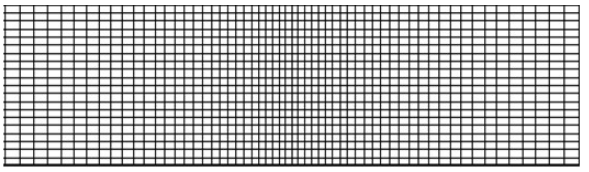

Fig. 2. *Schematic of grid*

Several different grid distributions were examined to ensure that the results are grid independent. For this purpose, the ferrofluid (water and 6 vol % Fe_3o_4) flow into a channel under a magnetic dipole with a strength of 0.1 Am and Reynolds number equal to 20 has been considered. Physical properties of the base fluid (water) and particles (Fe_3O_4) at the temperature of 25 ºC are presented in Table 1.

Table 1. *Properties of the water and magnetite*

property	water	Fe_3O_4
ρ	998.2 kg/m³	5200 kg/m³
C_p	4184.8 J/(kg K)	670 J/(kg K)
k	0.6 W/(m K)	6 W/(m K)
μ	0.001 kg/(m s)	-
diameter	0.2 nm	10 nm

The grid used for calculation has 300 and 90 nodes in the x and y directions, respectively. As shown in Table 2, a further increase of grid nodes does not affect the results.

Table 2. *Grid independent test*

	Node number ($x \times y$)	$\overline{Nu}$	$\overline{Ns}$
x	200×40	5.6415	0.3413
	300×40	5.4822	0.3597
	450×40	5.4513	0.3612
y	300×40	5.4513	0.3612
	300×60	5.7432	0.3584
	300×90	5.9084	0.3458
	300×135	5.9119	0.3441

Because the same lab work has not been done in this context, in order to demonstrate the validity and accuracy of numerical results, a comparison with the

previously published numerical work using a water-based ferrofluid with the following properties at 300 K reference temperature: $\rho = 1180\,kg/m^3$, $C_p = 4180\,J/(kgK)$, $\mu_0 = 0.001\,kg/(m \cdot s)$, $Pr = 5.5$ and $\chi_0 = 0.06$ under the influence of a line dipole has been done. The characteristic Reynolds number was $Re = 11.8$ and a comparison was performed for dipole strength of 0.19 Am. Fig. 3 indicates the comparison of the bulk temperature along the channel between the present work with the numerical ones of Ganguly et al. [2].

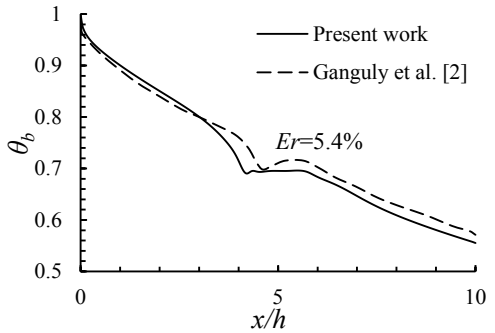

Fig. 3. *Comparison of the bulk temperature along the channel with same numerical results*

As seen, there is a good agreement between them and the average relative error (Er) is 5.4 %.

3 RESULTS AND DISCUSSION

In this work the forced flow of water-based ferrofluid consisting of 1 vol % to 6 vol % Fe_3O_4 particles with 10 nm mean diameter under the influence of a variable external magnetic field applied by a line dipole with dipole strength of 0.1 Am has been investigated numerically using control volume technique. The characteristic Reynolds number $Re = 20$ has been considered, so the flow regime is laminar. In the absence of the external magnetic field and zero volume fraction of magnetic nanoparticles, the forced flow reaches a hydro-dynamically fully developed profile at a length of $x/h = 2.284$ and achieves a constant velocity magnitude that is 1.5 times of the inlet ones. As the external magnetic field is applied, the kelvin body force overcomes the viscous force, and the fluid flow is strongly changed. Fig. 4a shows the kelvin body force distribution at 5 vol % Fe_3O_4. Vectors denote the kelvin body force direction while contours denote its magnitude. Furthermore, Fig. 4b demonstrate streamlines under the influence of external magnetic field at 5 vol % Fe_3O_4 particles.

Upstream of the dipole, the pressure-driven flow moves forward while a strong kelvin body force drives ferrofluid downward to the line dipole and causes significant momentum transfer toward the bottom wall. By moving ferrofluid toward the dipole at a distance of approximately 8 mm from the inlet ($x/h = 4$) Vertical flow barrier due to the magnetic field has been generated then it creates a flow pattern similar to being a vertical wall in a two-dimensional channel; thus, around the dipole a large vortex is formed. Downstream of the dipole, the kelvin body force resists the viscous force that moves the ferrofluid forward, so the fluid near bottom wall recirculate towards the dipole. Fig. 5 shows the velocity magnitude changes in the longitudinal direction at $y/h = 0.5$.

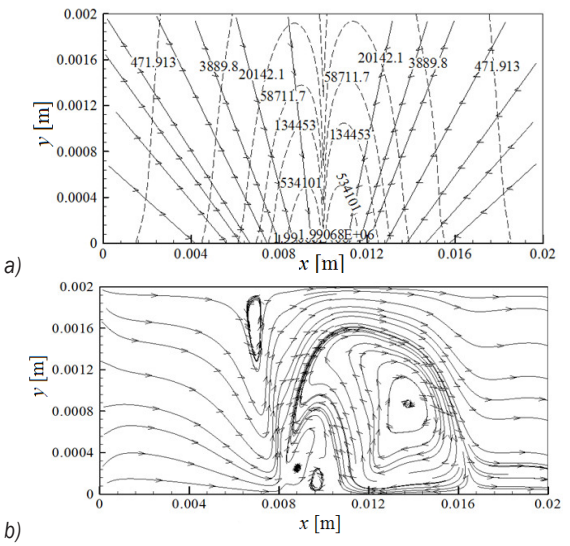

Fig. 4. *a) Kelvin body force distribution,* $(\boldsymbol{M} \cdot \nabla)\boldsymbol{B}$ *[N/m³], b) streamlines for 5 vol % Fe_3O_4 under influence of magnetic field*

As shown in Fig. 5, increasing the volume fraction of the Fe_3O_4 particles causes a slight reduction in the velocity magnitude at the inlet due to increasing the ferrofluid's density at a constant Reynolds number. Upstream the dipole, the velocity magnitude on the central line of channel reduces markedly because of the increasing kelvin body force by adding more volume fractions of Fe_3O_4 particles. As discussed, this force causes momentum transfer toward the bottom wall. Around the dipole, the vortex makes sinusoidal variations which their amplitude decreases gradually within approximately 8 mm after the dipole downstream and eventually a constant trend has been observed near the outlet. Owing to a larger kelvin body force caused by rising in the Fe_3O_4 volume fraction, more oscillations are observed in the velocity magnitude. The effect of Fe_3O_4 volume fraction on the kelvin body force in the longitudinal direction near the

bottom wall is presented in Fig. 6. As illustrated, the kelvin body force is symmetric about a vertical line passing through the dipole.

Applying the external magnetic field resulting from the dipole will increase the velocity and temperature gradients and leads to change in hydrodynamic and thermal parameters. Fig. 7 shows the variation of the friction factor on the bottom wall at different volume fractions.

It is seen that the friction factor has a relatively large amount at the inlet due to a high-velocity gradient. In the absence of an external magnetic field, the friction factor on the wall decreases along the channel length and reaches a constant amount in the hydrodynamic developed area. As said earlier, applying an external magnetic field while increasing Fe_3O_4 volume fraction will enhance the kelvin body force; thus, upstream the diploe the friction factor increases with a considerably sharp slope along the channel close to the dipole to reach a maximum value at the streamlines' jump due to the momentum transfer toward the bottom wall and consequently rising horizontal velocity gradient near the wall. Afterward, with a drop of the horizontal component of the velocity and upward ferrofluid flow, the friction factor diminishes such that reaches to the zero over the dipole. Downstream the dipole, first because of the backflow, friction factor becomes negative and finally away from dipole reaches to a constant positive amount near by the outflow. Fig. 8 depicts the effect of the Fe_3O_4 volume fraction on the average wall friction factor. As seen, with the increase in the Fe_3O_4 volume fraction, the mean wall friction factor enhances with a linear trend.

To characterize the overall effect of the Fe_3O_4 volume fraction on the pressure drop, the pumping work of the fluid $\dot{W}_p = \dot{m}\Delta p / \rho_{eff}$ (where $\dot{m} = \rho_{eff} u_\infty h$ and Δp is the total pressure difference between inlet and outlet) is presented in Fig. 9.

As seen, applying the external magnetic field enhances the required pumping work. Furthermore, the greater the volume fraction, the more pumping work is needed. Altering the flow field due to applying the magnetic field will cause to changes in temperature distribution. Fig. 10 shows the ferrofluid's temperature distribution under the influence of magnetic dipole strength $m = 0.1$ at 5 vol % Fe_3O_4.

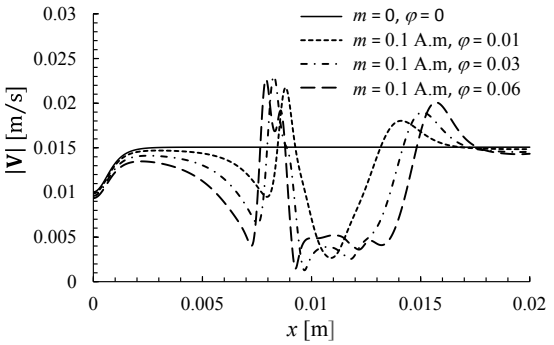

Fig. 5. *Comparison of the velocity magnitude in the longitudinal direction at y/h = 0.5 for different volume fractions.*

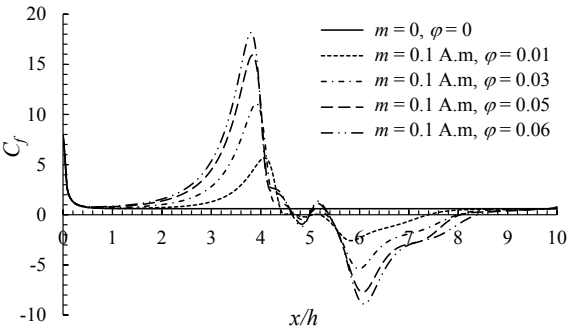

Fig. 7. *Variation of the wall friction factor along the channel length for different values of φ*

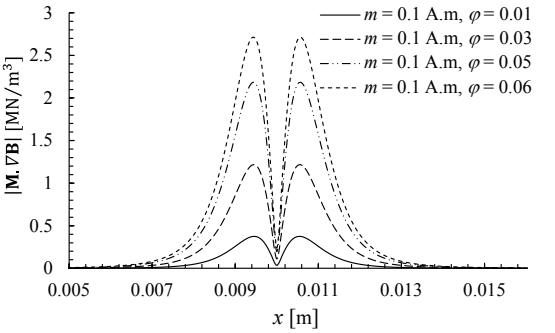

Fig. 6. *Variation of the kelvin body force along the channel length for different values of φ*

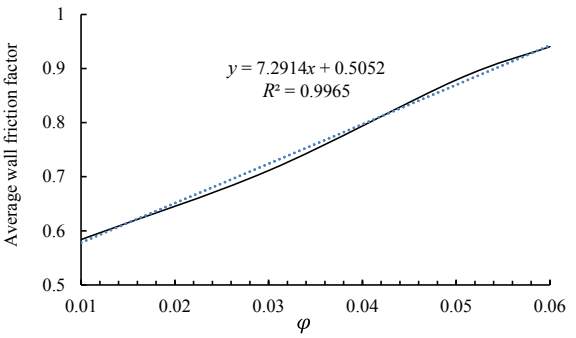

Fig. 8. *Variation of the average friction factor versus φ (m = 0.1 A m)*

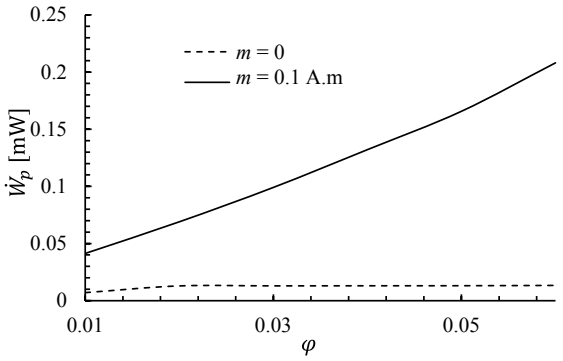

Fig. 9. *Effect of volume fraction on the pumping work*

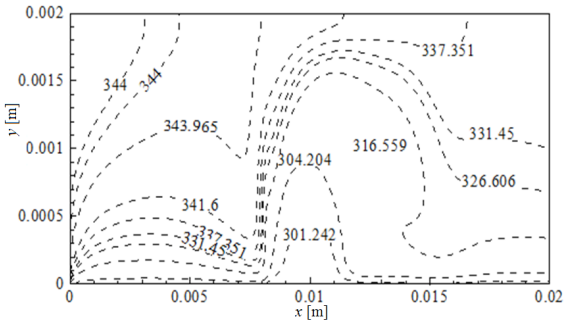

Fig. 10. *Temperature distribution at m = 0.1 and φ = 0.05*

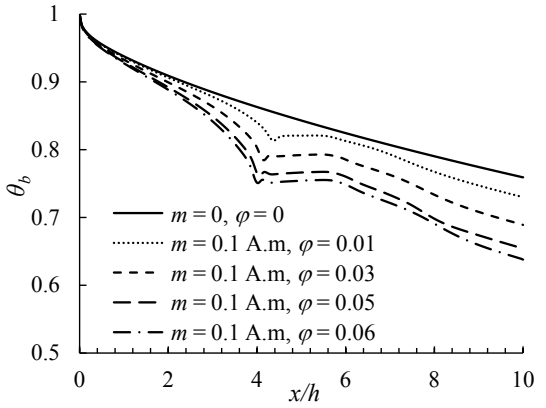

Fig. 11. *Variation of the bulk temperature along the channel length for different values of φ*

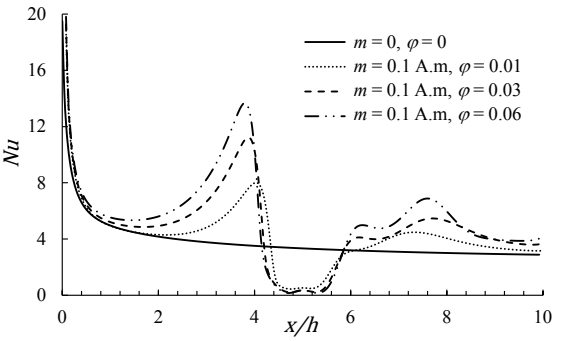

Fig. 12. *Variation of the local Nusselt number along the channel length at different volume fractions*

As the flow field changes, the temperature field is also altered accordingly such that a hump is made in the thermal boundary layer near the dipole. Upstream the dipole, the hot ferrofluid moves toward the bottom wall, and the thermal boundary-layer thickness is reduced. Due to the vertical motion of the ferrofluid before the dipole, the cold fluid near the downwall moves upward and downstream the diploe recirculates towards the dipole, so the thermal boundary-layer thickness Significantly increases. Fig. 11 indicates the variation of dimensionless bulk temperature along the channel length at different volume fractions.

As observed the bulk temperature is regularly reduced along the channel length in the absence of the magnetic field, while it will encounter a sudden drop around the dipole by adding magnetic nanoparticles and applying an external magnetic field. In fact, an augmentation in the Fe_3O_4 volume fraction creates a stronger vortex around the dipole, thus leading to an increase in heat transfer.

Altering the temperature distribution due to the exerted magnetic field causes changes in the temperature gradient within the ferrofluid. Thus, the convective heat transfer and the Nusselt number deals with change. Variation of *Nu* at different volume fractions is presented in Fig. 12.

In the absence of a magnetic field, the amount of *Nu* has been diminished from a maximum value at the inlet to 2.745 when *x*/*h* is 10. It is seen that exerting the magnetic field will increase the local *Nu* with a sharp slope upstream of the dipole. This is because of a high-temperature gradient at the wall, which has resulted in the reduction of the thermal boundary-layer thickness due to downward thermomagnetic convection. At the recirculation region above the dipole, colder ferrofluid formation prevents heat transfer; therefore, the local *Nu* is reduced. After this region, the thermal boundary-layer thickness decreases; the local *Nu* thus rises above the base fluid ones. An increase in the Fe_3O_4 volume fraction, causes the overall heat transfer and *Nu* to rise further from the base fluid. Fig. 13 depicts the effects of Fe_3O_4 volume fraction on the average Nusselt number. As seen, $\overline{Nu}$ is increased as more Fe_3O_4 particles is added, so that for 6 vol % Fe_3O_4, the $\overline{Nu}$ is enhanced by 51.1 % under the influence of the magnetic field and 8.5 % in the absence of a magnetic field in comparison to the base fluid.

The overall heat transfer is given by $Q = \dot{m} C_p \Delta T$, where ΔT is the bulk temperature difference between

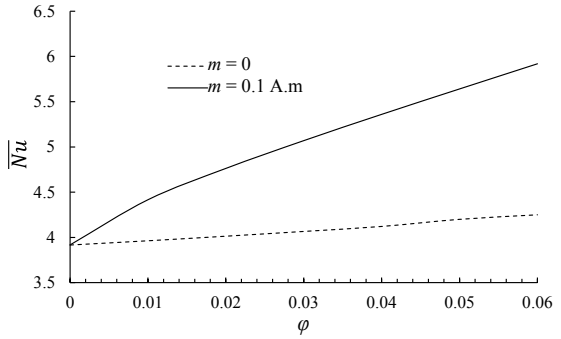

Fig. 13. *Effect of the Fe_3O_4 volume fraction on the average Nusselt number*

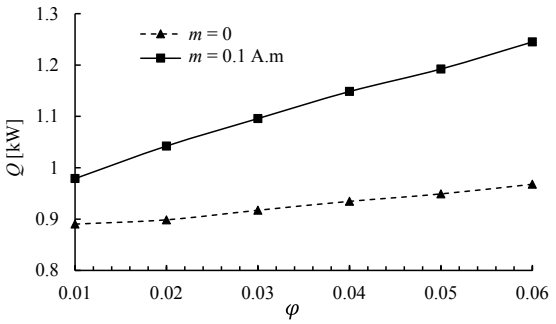

Fig. 14. *Effect of Fe_3O_4 volume fraction on the overall heat transfer*

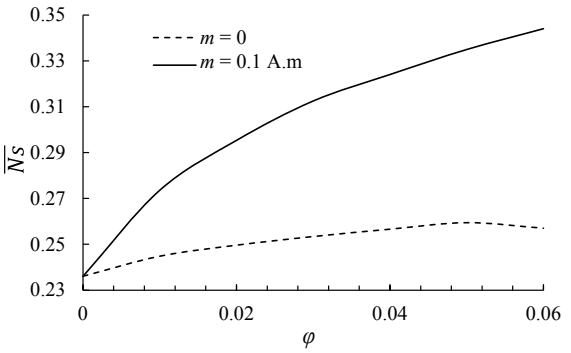

Fig. 15. *Effect of volume fraction on the average entropy generation*

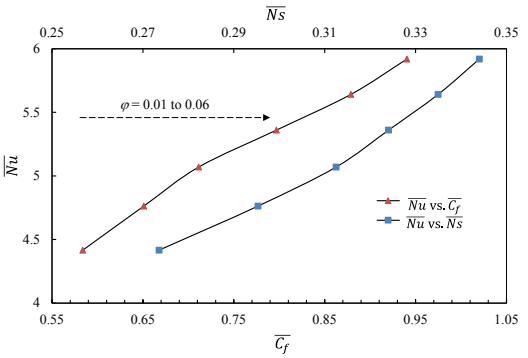

Fig. 16. *$\overline{Nu}$ versus $\overline{Ns}$ and $\overline{C}_f$ under magnetic dipole strength m = 0.1 A·m*

inlet and outlet. Fig. 14 shows the effect of Fe_3O_4 volume fraction on the overall heat transfer.

As illustrated the overall heat transfer increases by applying the external magnetic field, so that its maximum enhancement compared to the absence of a magnetic field accrues in 6 vol % Fe_3O_4 by 28.6%. Furthermore, the value of Q at 6 vol % with respect to 1 vol % Fe_3O_4 increases by 27.2% and 8.7% under magnetic dipole strength of m = 0.1 Am and without an external magnetic field, respectively. According to Figs. 9 and 14, the required pumping work can be neglected against the overall heat transfer.

The flow field and temperature distribution of ferrofluid is changed when an external magnetic field is applied; as a consequence of it, the velocity and temperature gradient of ferrofluid is altered. All these factors affect the entropy generation rate within the system. Fig. 15 depicts the effect of volume fraction on the average entropy generation. As seen, $\overline{Ns}$ increases with higher vol % of Fe_3O_4. Also applying the external magnetic field enhances $\overline{Ns}$ due to higher temperature and velocity gradients.

Fig. 16 shows the variation of $\overline{Nu}$ versus $\overline{Ns}$ and average wall friction factor under the influence of magnetic dipole strength m = 0.1 at different Fe_3O_4 volume fractions.

As seen, increasing nanoparticle volume fraction at the same time enhances $\overline{Nu}$, $\overline{Ns}$ and $\overline{C}_f$. In contrast, although adding nanoparticles to the base fluid increases the heat transfer rate, it also imposes an extra pumping work within the system and causes higher entropy generation. So the value of the solid volume fraction must be chosen so that the maximum heat transfer rate is obtained while having an optimum value of pumping work and entropy generation.

In order to have a better description for the effect of the Fe_3O_4 volume fraction on the thermomagnetic convection, the Nusselt number ratio and the entropy generation ratio have been developed as follows:

Nusselt number ratio:

$$NUR = \frac{\overline{Nu}}{\overline{Nu}_{m=0,\varphi=0,\mathrm{Re}=20}}, \tag{35}$$

entropy generation ratio:

$$NSR = \frac{\overline{Ns}}{\overline{Ns}_{m=0,\varphi=0,\mathrm{Re}=20}}. \tag{36}$$

Fig. 17 shows the effect of Reynolds number on the *NUR* and *NSR* within different Fe_3O_4 volume fraction under the influence of magnetic dipole strength $m = 0.1$.

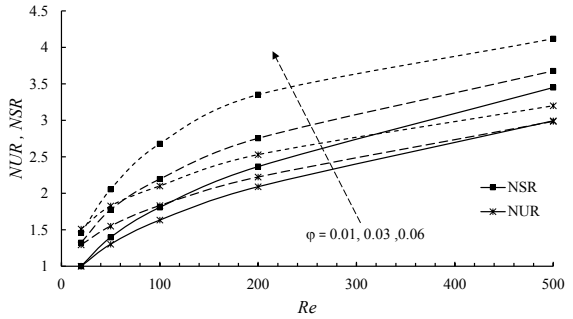

Fig. 17. *Effect of the Reynolds number and nanoparticles volume fraction on the NUR and NSR*

As expected, with an increase in the Reynolds number, both *NUR* and *NSR* enhance. Furthermore, a comparison has been carried out between different values of the Fe_3O_4 volume fractions. It is observed from Fig. 17 that using nanofluids at low Reynolds numbers have a good heat transfer performance while there is relatively less entropy generation.

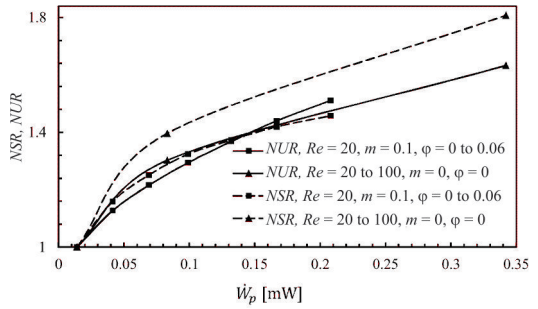

Fig. 18. *Comparison of the effect of base fluid Reynolds number and Fe_3O_4 volume fraction on the NUR and NSR*

Fig. 18 indicates the variation of *NUR* and *NSR* versus required pumping work for two cases of an accelerated base fluid without using nanoparticles and another non-accelerated nanofluid with different nanoparticle volume fractions of Fe_3O_4. As seen for a fixed value of the pumping work, at the low Reynolds numbers a slight increase in the base fluid *Re* (up to $Re = 60$) has a better effect on the heat transfer rate so that *NUR* for the accelerated base fluid is more than the non-accelerated nanofluid (volume fractions up to 0.04), but from the standpoint of thermodynamics causes higher entropy generation (more *NSR* compared to the non-accelerated nanofluid). At the higher values of the base fluid Reynolds number ($Re > 60$), the non-accelerated nanofluid with the volume fractions greater than 0.04 give a better heat transfer performance (more *NUR*) compared to the accelerated base fluid and also cause lower entropy generation.

With increased volume fraction of Fe_3O_4 up to 4 %, *NSR* within the system is greater than *NUR* while for the volume fractions between 0.04 and 0.06, this trend was reversed so that *NUR* at 6 vol % is enhanced by 10.4 % whereas *NSR* is increased by only 6.2 % compared to 4 vol % of the magnetic nanoparticles. This interesting result suggests that using volume fractions between 0.04 and 0.06, while increasing the convective heat transfer is also affordable, from the perspective of the second law of thermodynamics.

4 CONCLUSION

This paper represents a numerical investigation of laminar forced ferrofluid (consisting of water and Fe_3O_4 nanoparticles) flow through a tiny horizontal 2D channel by using the control volume technique. A line diploe was used to generate a non-uniform external magnetic field which is placed 1 mm below the lower channel wall halfway along the channel length. It was considered that the incompressible and viscous ferrofluid flow and the continuum flow assumption was satisfied. The effect of Fe_3O_4 volume fraction on the hydro-thermal parameters and entropy generation of the ferrofluid was studied.

- As the external magnetic field is applied, the kelvin body force overcomes the viscous force, so that the ferrofluid flow is strongly changed and a large vortex is formed around the dipole.
- Increasing the Fe_3O_4 volume fraction under the influence of the magnetic field causes more changes in the velocity and temperature fields, which leads to an obvious enhancement in the heat transfer.
- The required pumping work and average friction factor are enhanced by increasing the value of the Fe_3O_4 volume fraction.
- The average Nusselt number increases as more Fe_3O_4 particles are added, so that for 6 vol % Fe_3O_4, the $\overline{Nu}$ enhances by 51.1 % under the influence of the magnetic field and 8.5 % in the absence of a magnetic field in comparison to the base fluid.
- The results showed that the overall heat transfer is more affected in the presence of the external magnetic field, so that its value at 6 vol % with respect to 1 vol % Fe_3O_4 increases by 27.2 % and 8.7% under a magnetic dipole strength of

m = 0.1 Am and without an external magnetic field, respectively.

- The average entropy generation rises with higher vol % of Fe_3O_4, but the Nusselt number ratio at 6 vol % is enhanced by 10.4 % whereas entropy generation ratio increases by only 6.2 % compared to 4 vol % of the magnetic nanoparticles. This result emphasizes that using volume fractions ranging from 0.04 to 0.06 while increase the convective heat transfer, from the perspective of the second law of thermodynamics is also affordable.

6 NOMENCLATURE

a	x component of the dipole location [m]
$\boldsymbol{B}$	magnetic induction vector [T]
b	distance between the conductors [m]
C_f	friction factor
C_p	specific heat [J/(kg K)]
d	y component of the dipole location [m]
d_p	particle diameter [nm]
$\boldsymbol{H}$	magnetic field vector [A/m]
H_x	x component of magnetic field intensity [A/m]
H_y	y component of magnetic field intensity [A/m]
h	channel height [m]
I	current [A]
k	thermal conductivity [W/(m K)]
k_B	Boltzmann constant [1.3806503×10^{-23} J/K]
Kn	Knudsen number
L_s	characteristic channel length [m]
m	magnetic dipole moment per unit length [A·m]
$\boldsymbol{M}$	Magnetization vector [A/m]
m_p	particle magnetic moment [A·m²]
$\boldsymbol{V}$	velocity vector [m/s]
$\dot{W}_p$	pumping work [W]
x	axis in the Cartesian coordinate
y	axis in the Cartesian coordinate

Greek symbols

δ	Lattice spacing
ξ	Langevin parameter
θ	dimensionless temperature
λ	mean free path in a gas
μ	dynamic viscosity
μ_B	Bohr magneton
μ_0	magnetic permeability in vacuum
$\forall$	volume
Ms	saturation magnetization [A/m]
$\underline{Ns}$	Entropy generation number
$\overline{Ns}$	average entropy generation
NSR	entropy generation ratio
Nu	local Nusselt number
$\overline{Nu}$	average Nusselt number
NUR	Nusselt number ratio
P	pressure [Pa]
Pr	Prandtl number
Q	overall heat transfer [J/s]
$q_w^{"}$	wall heat flux [W/m²]
Re	Reynolds number
S_g	entropy generation [W/(m³K)]
S_{g0}	characteristic entropy generation
T	temperature [K]
u	x component of velocity [m/s]
v	y component of velocity [m/s]
ρ	Fluid density [kg/m³]
τ	shear stress
φ	volume fraction

Subscripts

b	pertaining to bulk fluid
c	pertaining to cold fluid
eff	effective
f	pertaining to base fluid
h	pertaining to hot fluid
m	mean value
p	pertaining to particle
0	pertaining to reference conditions
w	pertaining to wall

7 REFERENCES

[1] Cruz-Fierro, C.F. (2003). *Coupled Momentum and Heat Transport in Laminar Axisymmetric Pipe Flow of Ferrofluids in Non-Uniform Magnetic Fields: Theory and Simulation*. MSc Thesis, Oregon State University, Oregon.

[2] Ganguly, R., Sen, S., Puri, I.K. (2004). Heat transfer augmentation using a magnetic fluid under the influence of a line dipole. *Journal of Magnetism and Magnetic Materials*, vol. 271, no. 1, p. 63-73, **DOI:10.1016/j.jmmm.2003.09.015**.

[3] Bigdeli, M.B., Fasano, M., Cardellini, A., Chiavazzo, E., Asinari, P. (2016). A review on the heat and mass transfer phenomena in nanofluid coolants with special focus on automotive applications. *Renewable and Sustainable Energy Reviews*, vol. 60, pp. 1615-1633, **DOI:10.1016/j.rser.2016.03.027**.

[4] Gizzatov, A., Key, J., Aryal, S., Ananta, J., Cervadoro, A., Palange, A.L., Fasano, M., Stigliano, C., Zhong, M., Mascolo, D.D., Guven, A., Chiavazzo, E., Asinari, P., Liu, X., Ferrari, M., Wilson, L.J., Decuzzi, P. (2014). Hierarchically structured magnetic nanoconstructs with enhanced relaxivity and cooperative tumor accumulation. *Advanced Functional Materials*, vol. 24, p. 4584-4594, **DOI:10.1002/adfm.201400653**.

[5] Chiavazzo, E., Fasano, M., Asinari, P., Decuzzi P. (2014). Scaling behaviour for the water transport in nanoconfined geometries. *Nature Comunication*, 5:3565, **DOI:10.1038/ncomms4565**.

[6] Qian, S., Bau, H.H. (2009). Magneto-hydrodynamics based microfluidics. *Mechanics Research Communications*, vol. 36, no. 1, p. 10-21, **DOI:10.1016/j.mechrescom.2008.06.013**.

[7] Ibánez, G., Cuevas, S., López de Haro, M. (2006). Optimization of a magneto-hydrodynamic flow based on the entropy generation minimization method. *International Communications in Heat and Mass Transfer*, vol. 33, no. 3, p. 295-301, **DOI:10.1016/j.icheatmasstransfer.2005.12.003**.

[8] Finlayson, B.A. (1970). Convective instability of ferromagnetic fluids. *Journal of Fluid Mechanics*, vol. 40, no. 4, p. 753-767, **DOI:10.1017/S0022112070000423**.

[9] Tangthieng, C., Finlayson, B.A., Maulbetsch, J., Cader, T. (1999). Heat transfer enhancement in ferrofluids subjected to steady magnetic fields. *Journal of Magnetism and Magnetic Materials*, vol. 201, no. 1-3, p. 252-255, **DOI:10.1016/S0304-8853(99)00062-1**.

[10] Tzirtzilakis, E.E., Sakalis, V.D., Kafoussias, N.G., Hatzikonstantinou, P.M. (2004). Biomagnetic fluid flow in a 3D rectangular duct. *International Journal for Numerical Methods in Fluids*, vol. 44, no. 12, p. 1279-1298, **DOI:10.1002/fld.618**.

[11] Jafari, A., Tynjälä, T., Mousavi, S.M., Sarkomaa, P. (2008). Simulation of heat transfer in a ferrofluid using computational fluid dynamics technique. *International Journal of Heat and Fluid Flow*, vol. 29, no. 4, p. 1197-1202, **DOI:10.1016/j.ijheatfluidflow.2008.01.007**.

[12] Lajvardi, M., Moghimi-Rad, J., Hadi, I., Gavili, A., Dallali Isfahani, T., Zabihi, F., Sabbaghzadeh, J. (2010). Experimental investigation for enhanced ferrofluid heat transfer under magnetic field effect. *Journal of Magnetism and Magnetic Materials*, vol. 322, no. 21 p. 3508–3513, **DOI:10.1016/j.jmmm.2010.06.054**.

[13] Aminfar, H., Mohammadpourfard, M., Ahangar Zonouzi, S. (2013). Numerical study of the ferrofluid flow and heat transfer through a rectangular duct in the presence of a non-uniform transverse magnetic field. *Journal of Magnetism and Magnetic Materials*, vol. 327, p. 31-42, **DOI:10.1016/j.jmmm.2012.09.011**.

[14] Afrand, M., Farahat, S., Hossein Nezhad, A., Sheikhzadeh, G.A., Sarhaddi, F. (2014). Numerical simulation of electrically conducting fluid flow and free convective heat transfer in an annulus on applying a magnetic field. *Heat Transfer Research*, vol. 45, no. 8, p. 749-766, **DOI:10.1615/HeatTransRes.2014007285**.

[15] Afrand, M., Farahat, S., Hossein Nezhad, A., Sheikhzadeh, G.A., Sarhaddi, F. (2014). 3-D numerical investigation of natural convection in a tilted cylindrical annulus containing molten potassium and controlling it using various magnetic fields. *International Journal of Applied Electromagnetics and Mechanics*, vol. 46, no. 4, p. 809-821, **DOI:10.3233/JAE-141975**.

[16] Afrand, M., Farahat, S., Hossein Nezhad, A., Sheikhzadeh, G.A., Sarhaddi, F., Wongwises, S. (2015). Multi-objective optimization of natural convection in a cylindrical annulus mold under magnetic field using particle swarm algorithms. *International Communications in Heat and Mass Transfer*, vol. 60, p. 13-20, **DOI:10.1016/j.icheatmasstransfer.2014.11.006**.

[17] Mahmoodi, M., Esfe, M.H., Akbari, M., Karimipour, A., Afrand, M. (2015). Magneto-natural convection in square cavities with a source-sink pair on different walls. *International Journal of Applied Electromagnetics and Mechanics*, vol. 47, no. 1, p. 21-32, **DOI:10.3233/JAE-130097**.

[18] Malvandi, A., Safaei, M.R., Kaffash, M.H., Ganji, D.D. (2015). MHD mixed convection in a vertical annulus filled with Al203-water nanofluid considering nanoparticle migration. *Journal of Magnetism and Magnetic Materials*, vol. 382, p. 296-306, **DOI:10.1016/j.jmmm.2015.01.060**.

[19] Goshayeshi, H.R., Goodarzi, M., Safaei, M.R., Dahari, M. (2016). Experimental study on the effect of inclination angle on heat transfer enhancement of a ferrofluid in a closed loop oscillating heat pipe under magnetic field. *Experimental Thermal and Fluid Science*, vol. 74, p. 265-270, **DOI:10.1016/j.expthermflusci.2016.01.003**.

[20] Bejan, A. (1982). *Entropy Generation through Heat and Fluid Flow*, Wiley, New York.

[21] Mahian, O., Mahmud, Sh., Pop, I. (2012). Analysis of first and second laws of thermodynamics between two isothermal cylinders with relative rotation in the presence of MHD flow. *International Journal of Heat and Mass Transfer*, vol. 55, no. 17-18, p. 4808-4816, **DOI:10.1016/j.ijheatmasstransfer.2012.04.048**.

[22] Rashidi, M.M., Kavyani, N., Abelman, S. (2014). Investigation of entropy generation in MHD and slip flow over a rotating porous disk with variable properties. *International Journal of Heat and Mass Transfer*, vol. 70, p. 892-917, **DOI:10.1016/j.ijheatmasstransfer.2013.11.058**.

[23] Mojumder, S., Rabbi, Kh.Md., Saha, S., Hasan, M.N., Saha, S.C. (2016). Magnetic field effect on natural convection and entropy generation in a half-moon shaped cavity with semi-circular bottom heater having different ferrofluid inside. *Journal of Magnetism and Magnetic Materials*, vol. 407, p. 412-424, **DOI:10.1016/j.jmmm.2016.01.046**.

[24] Sharp, K.V., Adrian, R.J., Santiago, J.G., Molho, J.I. (2001). *Liquid Flows in Microchannels*. The MEMS Handbook, Gad-El-Hak, M. (ed.), CRC Press, Boca Raton, p. 6.1-6.38, **DOI:10.1201/9781420050905.ch6**.

[25] Shivakumara, I.S., Lee, J., Ravisha, M., Gangadhara Reddy, R. (2011). Effects of MFD viscosity and LTNE on the onset of ferromagnetic convection in a porous medium. *International Journal of Heat and Mass Transfer*, vol. 54, no. 11-12, p. 2630-2641, **DOI:10.1016/j.ijheatmasstransfer.2011.01.022**.

[26] Arikoglu, K., Ozkol, I., Komurgoz, G. (2008). Effect of slip on entropy generation in a single rotating disk in MHD flow. *Applied Energy*, vol. 85, no. 12, p. 1125-1236, **DOI:10.1016/j.apenergy.2008.03.004**.

[27] Batchelor, G.K. (1977). The effect of Brownian motion on the bulk stress in a suspension of spherical particles. *Journal of Fluid Mechanics*, vol. 83, no. 1, p. 97-117, **DOI:10.1017/S0022112077001062**.

[28] Hamilton, R.L., Crosser, O.K. (1962). Thermal conductivity of heterogeneous two-component system. *Industrial and Engineering Chemistry Fundamentals*, vol. 1, no. 3, p. 187-191, **DOI:10.1021/i160003a005**.

[29] Saleem, M., Anwar Hossain, Md., Mahmud, Sh., Pop, I. (2011). Entropy generation in Marangoni convection flow of heated fluid in an open ended cavity. *International Journal of Heat and Mass Transfer*, vol. 54, no. 21-22, p. 4473-4484, **DOI:10.1016/j.ijheatmasstransfer.2011.06.033**.